03

Optimized Monte Carlo Modeling of Coherent Optical Waves Propagation in Scattering Medium with Spatiotemporal Electric Field Tracking

© A. Doronin[1], I. Vladyko[1], E.V. Vasilieva[1], I.V. Meglinski[2]

[1] School of Engineering and Computer Science, Victoria University of Wellington, Wellington, New Zealand
[2] Aston Institute of Photonic Technologies, College of Engineering and Physical Sciences, Aston University, Birmingham, UK

e-mail: alex.doronin@vuw.ac.nz, vladykilya@myvuw.ac.nz, elena.vasilieva@vuw.ac.nz, i.meglinski@aston.ac.uk

Received June 07, 2025
Revised July 28, 2025
Accepted November 25, 2025

This work presents a novel, optimized Monte Carlo algorithm capable of accounting for the spatio-temporal evolution of the electric field, developed for highly accurate numerical modeling of coherent effects arising during the propagation of polarized optical radiation in turbid tissue-like scattering media. The method is based on the direct computation of successive changes in the electric field along photon trajectories within a scattering medium, enabling the simulation of interference, phase retardation, and polarization rotation caused by multiple scattering in optically inhomogeneous environments. The proposed algorithm is optimized for energy-efficient Apple M-series processors, leveraging unified memory and high-performance parallel computation of photon trajectories and electric field evolution for real-time simulation with low energy consumption. It is integrated into a previously developed open-access software that supports light propagation modeling with both temporal and spatial-polarization resolution, making it particularly attractive for a wide range of applications, including, notably, Mueller matrix polarimetry and interference-selective imaging with spatiotemporal signal filtering.

Keywords: polarized light, coherent effects, multiple scattering, method Monte Carlo, electric field tracking, Apple M-series processor, Parallel computing.

DOI: 10.61011/EOS.2025.12.63176.39-25

Introduction

Modeling the propagation of optical radiation in scattering media is critical in the study of fundamental effects arising from the interaction of coherent and polarized light with a complex randomly inhomogeneous structure such as biological tissue, including interference, phase shifts, depolarization, and speckle fluctuations [1]. In particular, for the analysis of interference, phase, and polarization transformations resulting from multiple scattering [2], the spatiotemporal characteristics of the vector electric field should be taken into account. Traditional models based on scalar approximation or the average intensity of [3–7] are insufficient to describe such effects. In this paper, we propose an improved numerical modeling algorithm based on the Monte Carlo method with direct calculation of the evolution of the electric field along the trajectories of photons in a scattering medium [8,9].

Modeling the interaction of light with biological tissues is critical for the development and design of diagnostic optical systems intended for non-invasive biomedical applications, and must take into account a number of technical parameters, including wavelength, polarization state, coherence, power of the detection radiation used, as well as the spatial configuration of the source–detector [6,7,10–15]. Ideally, a rigorous theoretical approach involves solving Maxwell's equations for the stochastic distribution of dielectric diffusers, followed by ensemble averaging over all possible implementations of the system. However, excessive computational costs and the complexity of the formulation of boundary conditions make this approach impractical for most real-world problems.

To solve this problem, the radiative transfer equation (RTE) has become widely used as an effective approximation for modeling the propagation of light in scattering media [16]. Among the most well-established methods of solving RTE, the Monte Carlo (MC) method can be distinguished — a stochastic, statistically reliable approach that has become the gold standard for modeling photon migration in turbid media [17,18]. In addition, numerous developments are currently underway aimed at expanding the MC method to include coherent and polarization-sensitive interaction mechanisms [8,11,19,20].

This paper presents a new improved MC model based on electric field tracking and designed to simulate the propagation of coherent polarized light in turbid scattering media. Unlike traditional scalar MC methods, the given approach explicitly tracks the evolution of the electric field vector of each photon packet as it passes through successive scattering acts. This vector formalism makes it possible to model such effects as polarization memory [21], cross-polarization dynamics, and coherence [22], which are usually neglected in the scalar models [3–7,11]. For the first time, the use of a specialized hardware architecture ensures the preservation

and access to localized space-time and three-dimensional volumetric information, such as photon trajectories and associated electric fields, throughout the entire process of the photons MC transfer. This option, which was previously difficult to achieve or inefficient in traditional CPU–GPU systems with separate memory pools, now provides a physically accurate and computationally efficient platform for modeling polarized light interactions in turbid media.

The algorithm originally presented by Kuzmin and Meglinsky [8,9,23], has been expanded and is now fully compatible with the hardware and runs directly on the energy-efficient Apple M processors which is consistent with the growing trend for development of portable high-performance biomedical computing platforms. Bridging the gap between traditional intensity-based MC simulations and full-wave and stringent electromagnetic methods [22,24], the developed method offers a highly accurate, but at the same time computationally accessible platform for modeling the light–tissue interactions. This study represents significant progress in modeling the transfer of polarized radiation for biomedical optics.

The basics of direct calculation of successive changes in the electric field along the trajectories of photons in a scattering medium

The MC method is recognized as the gold standard for modelling the light–tissue interactions due to its high accuracy and flexibility. First introduced and improved in the 1990s, the classic MC algorithm models the stochastic trajectories of photon packets as they pass through scattering, absorption, and reflection processes in complex media. In view of this, MC method gains to provide accurate reproduction and quantitative analysis of light localization in layered structures of model biological media, which has led to its widespread use in solving a wide range of optical tomography problems [26,27]. From a computational point of view, the MC method evaluates physical characteristics of the detected radiation by statistically selecting the most probable trajectories of photon packets, which makes it possible to model various spatiotemporal optical phenomena in detail. The scattering intensity of optical radiation propagating in the randomly inhomogeneous scattering media is outlined in this case on the basis of Bethe–Salpeter equation [8]:

$$G(\boldsymbol{R},\boldsymbol{R}_n;\boldsymbol{k}_i,\boldsymbol{k}_s)=\mu_s f(\boldsymbol{k}_i-\boldsymbol{k}_s)\delta(\boldsymbol{R}_n-\boldsymbol{R}_1)$$
$$+\mu_s\int f(\boldsymbol{k}_i-\boldsymbol{k}_{nj})\Lambda(\boldsymbol{R}_n-\boldsymbol{R}_j)G(\boldsymbol{R},\boldsymbol{R}_j;\boldsymbol{k}_{nj},\boldsymbol{k}_s)d\boldsymbol{R}_j, \quad (1)$$

where $G(\boldsymbol{R},\boldsymbol{R}_n;\boldsymbol{k}_i,\boldsymbol{k}_s)$ is Bethe–Salpeter equation propagator describing the field correlation. The wave vectors $\boldsymbol{k}_i$ and $\boldsymbol{k}_s$ represent the incident and scattered planar waves accordingly; μ_s — scattering coefficient. Propagator

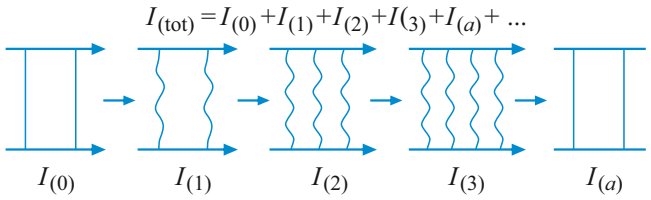

Figure 1. Schematic representation of ballistic photons $I_{(0)}$, one-time scattered $I_{(1)}$, twice scattered $I_{(2)}$, three-time scattered $I_{(3)}$, as well as photons that passed along the asymmetric trajectories $I_{(a)}$, as usually depicted on ladder diagrams in the context of multiple scattering theory.

describing the transfer between scattering events:

$$\Lambda(\boldsymbol{R})=R^2\exp\left(-\frac{R}{l}\right).$$

The phase function is defined by the following expression:

$$f(\boldsymbol{k}_s-\boldsymbol{k}_i)=\frac{\sigma(\boldsymbol{q})}{\int_{4\pi}d\Omega\,\sigma(\boldsymbol{q})}$$

with scattering vector $\boldsymbol{q}=\boldsymbol{k}_i-\boldsymbol{k}_s=2k\sin\left(\frac{\theta_s}{2}\right)$ and $\cos\theta_s=(\boldsymbol{k}_i-\boldsymbol{k}_s)\cdot\boldsymbol{k}_i/k^2$.

Iterating the Bethe–Salpeter equation, we obtain an expression for scattering contributions of higher orders:

$$G(\boldsymbol{R}_1,\boldsymbol{R}_n;\boldsymbol{k}_i,\boldsymbol{k}_s)=\mu_s f(\boldsymbol{k}_s-\boldsymbol{k}_i)\delta(\boldsymbol{R}_n-\boldsymbol{R}_1)$$
$$+\mu_s^2 f(\boldsymbol{k}_s-\boldsymbol{k}_{n1})\Lambda(\boldsymbol{R}_n)f(\boldsymbol{k}_{n1}-\boldsymbol{k}_i)+\mu_s^3 f(\boldsymbol{k}_s-\boldsymbol{k}_{n2})$$
$$\times\Lambda(\boldsymbol{R}_{n2})f(\boldsymbol{k}_{n2}-\boldsymbol{k}_{21})\Lambda(\boldsymbol{R}_{21})f(\boldsymbol{k}_{21}-\boldsymbol{k}_i)+\ldots. \quad (2)$$

Each term corresponds to one-, two-, three-fold, and subsequent orders of multiple scattering, which are stochastically taken into account in the analysis by MC method (Fig. 1).

In MC modeling, the distance that a photon travels between successive scattering acts obeys an exponential distribution [28]:

$$P(s)=\mu_t\exp(-\mu_t s), \quad (3)$$

where $\mu_t=\mu_s+\mu_a$ — extinction coefficient. Distance between the scattering acts is generated by formula:

$$s=-\frac{\ln\xi}{\mu_t}, \quad (4)$$

where $\xi\in(0,1)$ — an evenly distributed random number.

Thus, photon packets are injected into the medium from the surface, and their trajectories are iteratively updated until they are absorbed or leave the boundaries of the considered volume. Absorption is calculated by sequentially reducing the weight of the photon packet along the propagation path in the medium:

$$I=\sum_{j=1}^{N_{\mathrm{ph}}}W_j\exp\left(-\sum_{i=1}^{n_j}\mu_a l_i\right),$$

where W_j — statistical weight of j-th packet of photon, and l_i — length of i-th trajectory portion.

The polarization of an electromagnetic wave is usually described within the Stokes–Mueller or Jones formalism [29,30]. The Stokes vector and the Jones vector characterize the polarization state, while the Mueller and Jones matrices delineate the change in this state during scattering occurring because of fluctuations in the dielectric constant of the medium.

The Stokes–Mueller formalism is widely used for the analysis of polarization in birefringent turbid media in polarization-sensitive optical imaging [31]. In a number of experimental and numerical studies, characteristic polarization patterns in backscattering have been observed, represented as Mueller matrices [32,33]. It is demonstrated that the residual degree of polarization in the backscattered light is somewhat dependent on the optical properties of the scattering medium. In this view, let's consider a linearly polarized wave propagating along z axis with initial polarization along x axis. After scattering, the polarization vector $\boldsymbol{P}_i$ is determined according to the following expressions:

$$\boldsymbol{P}_i = -\boldsymbol{e}_i \times (\boldsymbol{e}_i \times \boldsymbol{P}_{i-1}) = (\mathbf{I} - \boldsymbol{e}_i \otimes \boldsymbol{e}_i)\boldsymbol{P}_{i-1}. \quad (6)$$

This can be represented in matrix form as:

$$\boldsymbol{P}_i = \begin{pmatrix} 1 - e_{iX}^2 & -e_{iX}e_{iY} & -e_{iX}e_{iZ} \\ -e_{iY}e_{iX} & 1 - e_{iY}^2 & -e_{iY}e_{iZ} \\ -e_{iZ}e_{iX} & -e_{iZ}e_{iY} & 1 - e_{iZ}^2 \end{pmatrix} \boldsymbol{P}_{i-1}. \quad (7)$$

Assuming that the initial polarization is $\boldsymbol{P}_0=\{1, 0, 0\}$, the final polarization after n scattering acts is defined as:

$$\boldsymbol{P}_n = \mathbf{P}_n\mathbf{P}_{n-1} \ldots \mathbf{P}_1\boldsymbol{P}_0. \quad (8)$$

In the scalar version of the polarized light propagation modelled by MC method, the parallel and orthogonal components of the scattered radiation are approximated based on the weighted contributions of photons detected by the detector. These components can be calculated as follows:

$$I_{XX}(\chi) = \sum_{j=1}^{N_{\text{ph}}} W_j \, \Gamma^{N_j} \, P_{XX,j}^2, \quad (9)$$

$$I_{XY}(\chi) = \sum_{j=1}^{N_{\text{ph}}} W_j \, \Gamma^{N_j} \, P_{XY,j}^2, \quad (10)$$

where $I_{XX}(\chi)$ and $I_{XY}(\chi)$ represent the scattering intensity with saved (parallel) and orthogonal polarization as a function of the scattering angle χ. Summation is made over all N_{ph} photon trajectories that have reached the detector. Here W_j — statistical weight of j-th photon accounting for the losses along its trajectory; N_j — number of scattering events experienced by this photon. The values $P_{XX,j}$ and $P_{XY,j}$ represent the polarization-dependent components of the phase function corresponding to scattering with parallel and orthogonal polarization, respectively.

The multiplier Γ characterizes the depolarizing contribution of each individual scattering event. It depends on the local scattering angle θ and is determined by the following expression:

$$\Gamma = \frac{2}{1 + \cos^2\theta}. \quad (11)$$

Such shape of Γ provides a more pronounced depolarization when scattering at large angles, which corresponds to the established physical patterns of light interaction with biological tissues, especially in anisotropic scattering modes [34,35].

The detected weight of the photon packet W_j is defined accounting for its coordinate $\mathbf{r}_D$:

$$W_j(\mathbf{r}_D) = W_0 \exp\left(-\sum_{i=1}^{N_j} \mu_{a,i}\ell_i\right), \quad (12)$$

where W_0 — initial weight of the photon (usually = 1), $\mu_{a,i}$ — absorption coefficient in i-th segment of the photon path, and ℓ_i — length of this segment. This exponential decay simulates the cumulative absorption effect along the photon trajectory.

Modelling in practice using Apple ARM-processors

The advent of high-performance parallel computing platforms has significantly transformed the MC method, making it possible to significantly reduce calculation time and simulate complex light–tissue interactions with increased detail and physical dependability [6,7,36]. This progress has contributed to significant advances in biomedical optics, providing opportunities for deeper analysis of spectral characteristics and polarization-dependent effects, including the development of modern image reconstruction algorithms using machine learning methods [14,22,37–49]. Yet, modeling the coherent propagation of polarized light in scattering biological media remains the most resource-intensive task, especially in tasks involving the study of the formation and spatiotemporal localization of optical radiation, taking into account birefringence or polarization-dependent detection geometry [14,41].

To solve this problem, we present an energy-efficient MC algorithm with tracking the evolution of the electric field vector during photon migration in scattering (turbid) media. Developed based on Apple M processors architecture, this method provides highly detailed modeling of polarization-resolved radiation transfer in multilayer biological tissues (Fig. 2). The algorithm tracks the electric field vector $\boldsymbol{P}$ of each photon packet, iteratively updating it in accordance with each act of scattering. The proposed approach provides an accurate reproduction of the effects of depolarization, co- and cross-polarized scattering, as well as the polarization memory effect [22,50].

At the beginning of the modeling, photon packets are initialized with the spatial and angular profile of the

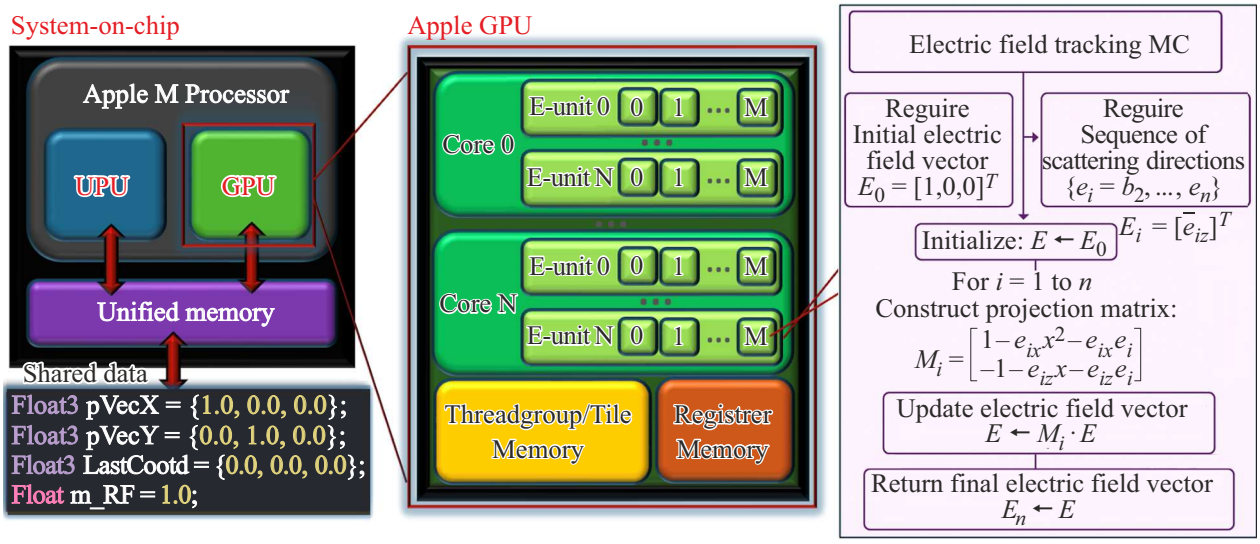

Figure 2. A schematic representation of the implementation of MC algorithm, which takes into account successive changes in the electric field along the trajectories of photon packets, based on Apple M system-on-a-chip architecture. Updates of the polarization vectors with appropriate scattering actions are mapped to GPU execution threads by using unified memory and parallel processing at the level of Apple GPU thread groups to ensure efficient data access and high computational performance.

Comparison of the results of modeling by MC method with Milne's analytical solution and the results of alternative numerical modeling [51,52]. The table includes the components of both, linear intensity ($I_{\parallel}, I_{\perp}$), and circular intensity ($I_{\text{co}}, I_{\text{cross}}$) of polarization, as well as their ratio

Source	$I_{\parallel}$	$I_{\perp}$	$I_{\parallel}/I_{\perp}$	I_{co}	I_{cross}	$I_{\text{co}}/I_{\text{cross}}$
Milne solution [51,52]	3.025	1.563	1.935	1.751	2.837	0.617
Kuzmin et al. [51,52]	3.029	1.570	1.929	1.758	2.841	0.618
Present model	3.023	1.566	1.930	1.753	2.838	0.617

Gaussian beam. Their initial coordinates (x, y, z), guide cosines (u_x, u_y, u_z), and polarization vectors $\boldsymbol{P}_0$ are set in the Cartesian coordinate system. As it propagates, each act of scattering causes a deterministic transformation of the current polarization vector $\boldsymbol{P}_i$ in accordance with the following expression:

$$\boldsymbol{P}_i = (\mathbf{I} - \boldsymbol{e}_i \otimes \boldsymbol{e}_i)\boldsymbol{P}_{i-1}, \tag{13}$$

where $\boldsymbol{e}_i$ — unit vector specifying the new direction of propagation after i^{th}-th act of scattering, and $\mathbf{I}$ — unit matrix. This transformation ensures a consistent evolution of polarization along the photon trajectory, taking into account the scattering geometry and the anisotropy of the medium.

Photon interactions are described by the probabilities of elastic scattering P_{Elastic} and absorption P_{Abs}, determined by the optical properties of the medium: scattering coefficients μ_s and absorption μ_a. The photon displacement step Δr is selected less than the minimum free path to ensure correct sampling of interaction events. At each calculation step, the probability of a specific interaction is calculated as follows:

$$P_i = 1 - e^{-\Delta r / l_i}, \tag{14}$$

where l_i denotes the average free path length for the corresponding type of interaction.

Here, Metal technology from Apple is used to accelerate calculations made by the graphic processor. Each GPU thread processes individual photon packet providing full computational independence. Apple M architecture with a unified memory minimizes the delays between CPU and GPU, providing efficient access to the general memory when tracing the photons packet. The state of each photon packet, including trajectory, statistical weight, and polarization vector, is stored in device registers or memory buffers optimized for vectors (SIMD). Photon packet propagation is carried out within the iterative cycle of the core. At each step, the state of the photon packet is updated according to the interaction probabilities. The absorbed parts of the photon packet are marked to complete their further modeling, and their energy contribution is registered. Photon packets after scattering change their direction according to Heney–Greenstein phase function; their polarization vector is updated accordingly, as described above. The polarization states are continuously monitored, which makes it possible to accurately reconstruct the intensity distributions corresponding to the components

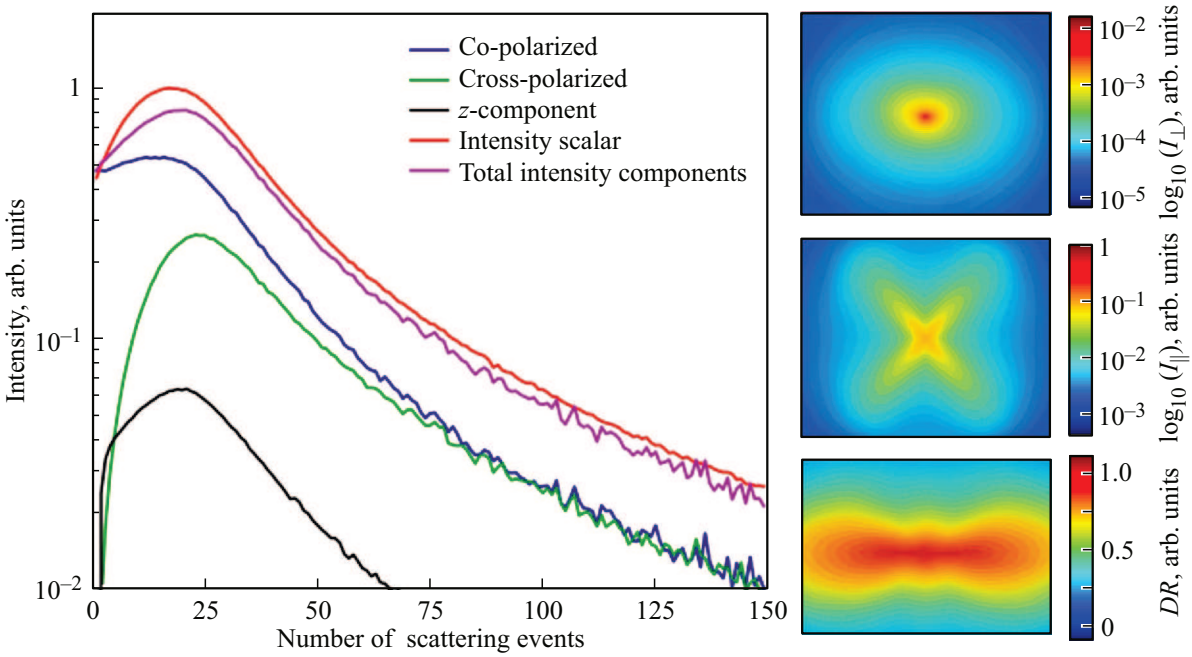

Figure 3. The results of MC-modelling of the propagation of polarized light in a turbid medium with anisotropy factor $g = 0.9$ and scattering coefficient $\mu_s = 30\,\text{mm}^{-1}$. On the left: intensity versus the number of scattering events for parallel polarized ($I_\parallel$), perpendicular polarized ($I_\perp$) components, as well as for scalar intensity (red curve) and total vector intensity (magenta curve). On the right: spatial distributions of the polarization-resolved parameters: at the top — parallel polarized intensity $I_\parallel$; in the center $\log_{10}$ perpendicular to the polarized intensity $I_\perp$; at the bottom — spatial distribution of the depolarization coefficient (DR), reflecting spatial variations of polarization conservation during multiple scattering.

with saved and changed polarization. Photon packets that exceed the permissible spatial or angular range are excluded from further modeling. Thus, a spatially resolved intensity distribution is formed at the output, taking into account the polarization characteristics of the detected radiation.

Results and discussion

The findings obtained from using the proposed MC model in the table below are in good consistency with both, the results of Milne analysis, and the numerical data provided by V.L. Kuzmin et al. [9,23]. For example, the calculated ratio $I_\parallel/I_\perp$ is close to the values of 1.935 (according to Milne) and 1.929 (according to Kuzmin's method), which confirms the high accuracy of polarization-dependent intensity modeling. Similarly, the ratio I_{co}/I_{cross}, which describes the behavior of circular polarization, exactly corresponds to the analytical value of 0.617, which additionally proves the correctness of describing coherent effects in the proposed approach.

The comparison results confirm the numerical dependability of the developed MC model, taking into account the evolution of the electric field, and demonstrate its high accuracy in reproducing polarization effects. Moreover, the model correctly reproduces the phenomena of spiral inversion and spatial characteristics of optical radiation depolarization [53–55].

To validate performance of the improved MC model, taking into account the evolution of the electric field (MC model with EP), the spatial and volumetric distributions of key polarization-resolved quantities in a highly scattering anisotropic medium were calculated. As shown in Figure 3, the results obtained show excellent consistency with the expected physical behavior, including the memory effect of polarization and characteristic patterns of depolarization [53–56]. In particular, the model successfully reproduces parallel polarized ($I_\parallel$) and perpendicular polarized ($I_\perp$) intensity components, as well as the depolarization coefficient (DR) over a wide scattering range. The data obtained provide a detailed understanding of the spatial structure of backscattered light [55,57] and quantify the degree of preservation or loss of polarization as a result of multiple scattering in media with high anisotropy $g = 0.9$ and scattering coefficient $\mu_s = 30\,\text{mm}^{-1}$ [22,43,57]. The ability of the model to accurately reproduce such distributions confirms its physical validity and practical value for numerical analysis of light interaction with biological tissues.

To assess the performance of the implemented improved MC model, we conducted extensive testing with an emphasis on computational speed, energy efficiency, and numerical stability. First of all, the throughput capacity was compared by the number of processed photons: the efficiency of the Metal-accelerated implementation was evaluated compared to previously developed Monte Carlo algorithms based on NVIDIA CUDA and classical CPUs. The results

demonstrated impressive performance: the proposed model is capable of processing from 2 million photons per second (on M1 Pro chip) to 5 million photons per second (on M2 chip) in a homogeneous medium. This bandwidth makes it possible to conduct large-scale modeling of the order of 10^{11} photonic packets in a reasonable time, which was previously achievable only when using high-performance clusters with graphics accelerators. The findings convincingly demonstrate that the developed model may find its application in the portable and high-speed biomedical optics in real time.

Existing solutions based on high-performance NVIDIA GPUs, for example, within CUDA platform [6,7], do provide higher absolute throughput — approximately 2.3 times higher. However, this is accompanied by significantly higher energy consumption. Thus, GeForce RTX 3090 graphics card is capable of processing about twice as many photons per second, but its power consumption under load reaches 360W, while the M1 Pro graphics processor consumes only about 10W. Overall computational efficiency is determined not only by raw performance indicators, but also depends on many factors, including the algorithm structure, hardware architecture, software interfaces used, and the development environment.

It should be noted that the presented implementation of the MC algorithm is specially optimized for Apple M processors using Metal computing platform. However, the algorithm itself is not strictly tied to Apple hardware. Key architectural features that ensure its efficiency, such as ARM processors and unified memory, are becoming increasingly common on other platforms, including Qualcomm Snapdragon processors and other ARM-compatible solutions. If there is support for similar computing APIs, as well as access to unified memory, the developed MC algorithm can be adapted to the appropriate computing platform. Thus, although Apple hardware was used in this study due to its affordable energy-efficient architecture and native Metal support, the MC algorithm itself and its conceptual structure are transferrable and not limited to a specific hardware.

Conclusions

This paper presents a new optimized MC algorithm with the ability to take into account the spatiotemporal dynamics of the electric field [58], developed for the most accurate computational modeling of coherent effects arising from the propagation of polarized optical radiation in scattering media. Unlike traditional scalar MC modeling methods, the developed algorithm provides a physically correct description of coherent optical effects, including polarization, interference, and absorption, by sequentially calculating changes in the vector electric field along photon trajectories in a scattering medium. The presented MC algorithm is optimized for energy-efficient Apple M processors using GPU acceleration, which allows high-performance modeling on portable computer platforms. The algorithm was validated by comparing it with Milne's analytical solution and numerically oriented reference MC models. The results obtained are in good agreement with the results of reference calculations of the spatial distribution of the scattered radiation intensity and the depolarization coefficients, confirming the adequacy of applicability of the model in polarization-sensitive configurations. The algorithm is integrated into a previously developed software module with open access to the source code [59], which supports modeling light propagation with both temporal and spatial-polarizing resolution. The module combines computational efficiency with physical reliability and can be expanded to solve a wide range of tasks, including speckle analysis, coherent-selective visualization, and time-resolved light transfer modeling. The proposed optimized MC method is a reliable and scalable platform for computational modeling of the interaction of light with inhomogeneous media, including biological tissues. The method is intended for use in the next-generation optical technologies such as diffusion-wave optical coherence spectroscopy [60,61] and phase-polarization-sensitive optical biopsy [47,62].

Acknowledgments

The authors of this paper express their deep gratitude to professor V.L. Kuzmin for his fundamental theoretical research and key contribution to the initial implementation of the Monte Carlo algorithm using C/C++ programming language. This contribution became the basis for and largely predetermined further development of computational modeling methods for the propagation of coherent polarized optical radiation in random media, taking into account the spatiotemporal dynamics of the electric field and the possibility of studying the effects associated with the orbital angular momentum (OAM) [41,45].

Conflict of interest

The authors declare that they have no conflict of interest.

References

[1] V.L. Kuz'min, I.V. Meglinski. Quant. Electron., **36** (11), 990 (2006). DOI: 10.1070/QE2006v036n11ABEH013338
[2] I.V. Meglinski, V.V. Tuchin. Dokl. Phys., **524**, 23–32 (2025). DOI: 10.7868/S3034508125050044
[3] S.T. Flock, M.S. Patterson, B.C. Wilson, D.R. Wyman. IEEE Trans. Biomed. Eng., **36** (12), 1162–1168 (1989). DOI: 10.1109/10.42107
[4] L. Wang, S. Jacques. J. Opt. Soc. Am. A, **10** (8), 1746–1752 (1993). DOI: 10.1364/JOSAA.10.001746
[5] L. Wang, S.L. Jacques, L. Zheng. Comput. Methods Programs Biomed., **47** (2), 131–146 (1995). DOI: 10.1016/0169-2607(95)01640-F
[6] I.V. Meglinski, A. Doronin. SPIE Newsroom (2011). DOI: 10.1117/2.1201110.003879
[7] A. Doronin, I.V. Meglinski. J. Biomed. Opt., **17** (9), 090504 (2012). DOI: 10.1117/1.JBO.17.9.090504

[8] I.V. Meglinski, V.L. Kuzmin, D.Y. Churmakov, D.A. Greenhalgh. Proc. R. Soc. A, **461**, 43–53 (2005). DOI: 10.1098/rspa.2004.1369
[9] V.L. Kuz'min, I.V. Meglinski. JETP Lett., **79** (3), 109–112 (2004). DOI: 10.1134/1.1719124
[10] H.H. Barrett, K.J. Myers. *Foundations of Image Science* (Wiley-Interscience, Hoboken, NJ, 2004).
[11] S.V. Gangnus, S.J. Matcher, I.V. Meglinski. Laser Phys., **14**, 886–891 (2004).
[12] I.V. Meglinski, A.V. Doronin, A.N. Bashkatov, E.A. Genina, V.V. Tuchin. In: *Computational Biophysics of the Skin,* ed. by B. Querleux (Pan Stanford Publishing, Singapore, 2014), ch. 2, p. 25–56.
[13] A.V. Bykov, A.V. Doronin, I.V. Meglinski. In: *Deep Imaging in Tissue and Biomedical Materials,* ed. by L. Shi, R.R. Alfano (Jenny Stanford Publishing, Singapore, 2017), p. 295–322.
[14] A.V. Doronin, C.M. Macdonald, I.V. Meglinski. J. Biomed. Opt., **19** (2), 025005 (2014). DOI: 10.1117/1.JBO.19.2.025005
[15] A. Doronin, I. Fine, I.V. Meglinski. Laser Phys., **21**, 1972–1977 (2011). DOI: 10.1134/S1054660X11190078
[16] S. Chandrasekhar. *Radiative Transfer* (Dover Publications, N.Y., 1960).
[17] I.V. Meglinski. Quant. Electron., **31** (12), 1101–1107 (2001). DOI: 10.1070/QE2001v031n12ABEH002108
[18] E. Berrocal, D.Y. Churmakov, V.P. Romanov, M.C. Jermy, I.V. Meglinski. Appl. Opt., **44**, 2519–2529 (2005). DOI: 10.1364/AO.44.002519
[19] J.C. Ramella-Roman, S.A. Prahl, S.L. Jacques. Opt. Express, **13** (12), 4420–4438 (2005). DOI: 10.1364/OPEX.13.004420
[20] J.C. Ramella-Roman, S.A. Prahl, S.L. Jacques. Opt. Express, **13** (26), 10392–10405 (2005). DOI: 10.1364/OPEX.13.010392
[21] C.M. Macdonald, S.L. Jacques, I.V. Meglinski. Phys. Rev. E, **91**, 033204 (2015). DOI: 10.1103/PhysRevE.91.033204
[22] A. Doronin, A.J. Radosevich, V. Backman, I.V. Meglinski. J. Opt. Soc. Am. A, **31** (11), 2394–2400 (2014). DOI: 10.1364/JOSAA.31.002394
[23] V.L. Kuz'min, I.V. Meglinski. Opt. Commun., **273** (2), 307–310 (2007). DOI: 10.1016/j.optcom.2007.01.025
[24] R. Rowland, A. Ponticorvo, M.L. Baldado, G.T. Kennedy, D.M. Burmeister, R.J. Christy, N.P. Bernal, A.J. Durkin. J. Biomed. Opt., **24** (5), 056007 (2019). DOI: 10.1117/1.JBO.24.5.056007
[25] S.L. Jacques. J. Biomed. Opt., **27** (8), 083002 (2022). DOI: 10.1117/1.JBO.27.8.083002
[26] A.F. Peña, A. Doronin, V.V. Tuchin, I.V. Meglinski. J. Biomed. Opt., **19**, 086002 (2014). DOI: 10.1117/1.JBO.19.8.086002
[27] A.F. Peña, J. Devine, A. Doronin, I.V. Meglinski. Opt. Lett., **38** (14), 2629–2631 (2013). DOI: 10.1364/OL.38.002629
[28] I.M. Sobol'. *The Monte Carlo Method* (University of Chicago Press, Chicago, 1974).
[29] C. Brosseau. *Fundamentals of Polarized Light: a Statistical Optics Approach* (John Wiley & Sons, N.Y., 1998).
[30] C.F. Bohren, D.R. Huffman. *Absorption and Scattering of Light by Small Particles* (Wiley, N.Y., 1983).
[31] X. Wang, L.V. Wang. J. Biomed. Opt., **7**, 279–290 (2002). DOI: 10.1117/1.1483315
[32] S. Bartel, A.H. Hielscher. Appl. Opt., **39**, 1580–1588 (2000). DOI: 10.1364/AO.39.001580
[33] M.J. Rakovic, G.W. Kattawar, M. Mehrubeoglu, B.D. Cameron, L.V. Wang, S. Rastegar, G.L. Cote. Appl. Opt., **38**, 3399–3408 (1999). DOI: 10.1364/AO.38.003399
[34] V.V. Tuchin. *Tissue Optics: Light Scattering Methods and Instruments for Medical Diagnosis,* 3rd ed. (SPIE Press, Bellingham, 2015). DOI: 10.1117/3.1003040
[35] V.V. Tuchin. *Handbook of Optical Biomedical Diagnostics,* vol. 2: Methods, 2nd ed. (SPIE Press, Bellingham, 2016). DOI: 10.1117/3.2219608
[36] E. Alerstam, T. Svensson, S. Andersson-Engels. J. Biomed. Opt., **13** (6), 060504 (2008). DOI: 10.1117/1.3041496
[37] A. Clennell, V. Nguyen, V.V. Yakovlev, A. Doronin. Opt. Express, **31** (19), 30921–30931 (2023). DOI: 10.1364/OE.496516
[38] I.V. Meglinski, S.J. Matcher. Comput. Methods Programs Biomed., **70** (2), 179–186 (2003). DOI: 10.1016/S0169-2607(02)00099-8
[39] G.I. Petrov, A. Doronin, H.J.T. Whelan, I.V. Meglinski, V.V. Yakovlev. Biomed. Opt. *Express,* **3**, 2154–2161 (2012). DOI: 10.1364/BOE.3.002154
[40] A. Doronin, V. Yakovlev, V.S. Bagnato. *Biomed. Opt. Express,* **15**, 1682–1693 (2024). DOI: 10.1364/BOE.514003
[41] A. Doronin, N. Vera, J.P. Staforelli, P. Coelho, I.V. Meglinski. Photonics, **6** (2), 56 (2019). DOI: 10.3390/photonics6020056
[42] V.V. Dremin, Z. Marcinkevics, E.A. Zherebtsov, A. Popov, A. Grabovskis, H. Kronberga, K. Geldnere, A. Doronin, I.V. Meglinski, A.V. Bykov. IEEE Trans. Med. Imaging, **40**, 1207–1216 (2021). DOI: 10.1109/TMI.2021.3049591
[43] A. Doronin, L. Tchvialeva, I. Markhvida, T.K. Lee, I.V. Meglinski. J. Biomed. Opt., **21**, 071117 (2016). DOI: 10.1117/1.JBO.21.7.071117
[44] E.A. Zherebtsov, V.V. Dremin, A.P. Popov, A. Doronin, D.A. Kurakina, M.Yu. Kirillin, I.V. Meglinski, A.V. Bykov. Biomed. Opt. Express, **10** (7), 3545–3559 (2019). DOI: 10.1364/BOE.10.003545
[45] F. Khanom, N. Mohamed, I. Lopushenko, A.Yu. Sdobnov, A. Doronin, A. Bykov, E.U. Rafailov, I. Meglinski. Sci. Rep., **14** (1), 20662 (2024). DOI: 10.1038/s41598-024-70954-x
[46] D. Robinson, K. Hoong, W. Kleijn, A. Doronin, J. Rehbinder, J. Vizet, A. Pierangelo, T. Novikova. J. Biomed. Opt., **28**, 102904 (2023). DOI: 10.1117/1.JBO.28.10.102904
[47] A. Ushenko, A. Sdobnov, I. Soltys, Y. Ushenko, A. Dubolazov, V. Sklyarchuk, A. Olar, L. Trifonyuk, A. Doronin, W. Yan, A. Bykov, I. Meglinski. Sci. Rep., **14** (1), 13679 (2024). DOI: 10.1038/s41598-024-63816-z
[48] S. Chae, T. Huang, O. Rodríguez-Núñ ez, T. Lucas, J. Vanel, J. Vizet, A. Pierangelo, G. Piavchenko, T. Genova, A. Ajmal, J. Ramella-Roman, A. Doronin, H. Ma, T. Novikova. IEEE Trans. Med. Imaging (2025). DOI: 10.1109/TMI.2025.3567570
[49] I. Meglinski, C. Macdonald, A. Doronin, M. Eccles. In: *Optics in the Life Sciences* (Optica Publishing Group, 2013), p. BM2A.4. DOI: 10.1364/BODA.2013.BM2A.4
[50] M. Xu, R.R. Alfano. Phys. Rev. E, **72**, 065601 (2005). DOI: 10.1103/PhysRevE.72.065601
[51] V.L. Kuzmin, E. Aksenova. J. Exp. Theor. Phys., **96** (5), 816–831 (2003). DOI: 10.1134/1.1581936
[52] V.L. Kuzmin. Opt. Spectrosc., **93** (3), 439–448 (2002). DOI: 10.1134/1.1509828
[53] I. Meglinski, V.L. Kuzmin. Prog. Electromagn. Res. M, **16**, 47–61 (2011). DOI: 10.2528/PIERM10102106
[54] V.L. Kuz'min, I.V. Meglinski. J. Exp. Theor. Phys., **110** (5), 742–753 (2010). DOI: 10.1134/S1063776110050031.

[55] I. Lopushenko, A. Bykov, I. Meglinski. Phys. Rev. A, **108**, L041502 (2023). DOI: 10.1103/PhysRevA.108.L041502
[56] C. Macdonald, I. Meglinski. Laser Phys. Lett., **8** (4), 324–328 (2011). DOI: 10.1002/lapl.201010133
[57] I. Lopushenko, O. Sieryi, A. Bykov, I. Meglinski. J. Biomed. Opt., **29** (5), 052913 (2024). DOI: 10.1117/1.JBO.29.5.052913
[58] A. Doronin. Monte Carlo models and code [Electronic resource]. URL: https://github.com/aledoronin/ (date of access: 2025).
[59] A. Doronin. Cloud based Monte Carlo platform for the needs of Biophotonics, Biomedical Optics and Computer Graphics [Electronic resource]. URL: https://www.lighttransport.net/ (date of access: 2025).
[60] A. Sdobnov, G. Piavchenko, A. Bykov, I. Meglinski. Laser Photonics Rev., **18** (2), 2300494 (2024). DOI: 10.1002/lpor.202300494
[61] E. Zherebtsov, A. Sdobnov, O. Sieryi, M. Kaakinen, L. Eklund, T. Myllyl, A. Bykov, I. Meglinski. Laser Photonics Rev., **19** (2), 2401016 (2025). DOI: 10.1002/lpor.202401016
[62] I. Meglinski, I. Lopushenko, A. Sdobnov, A. Bykov. Opt. Photonics News, **12**, 43 (2024).

Translated by J.Savelyeva